東北大学機関リポジトリ
TOUR
Tohoku University Repository

Decreased hydrogen content in diamond-like carbon grown by CH4/Ar photoemission-assisted plasma chemical vapor deposition with CO2 gas

著者	Shuichi Ogawa, Rintaro Sugimoto, Nobuhisa Kamata, Yuji Takakuwa
journal or publication title	Surface and Coatings Technology
volume	350
page range	863-867
year	2019-04-10
URL	http://hdl.handle.net/10097/00127712

doi: 10.1016/j.surfcoat.2018.04.016

Creative Commons : 表示 - 非営利 - 改変禁止
http://creativecommons.org/licenses/by-nc-nd/3.0/deed.ja

This is the peer reviewed version of the following article:

S. Ogawa, R. Sugimoto, N. Kamata, Y. Takakuwa (2018) “Decreased hydrogen content in diamond-like carbon grown by CH_4/Ar photoemission-assisted plasma chemical vapor deposition with CO_2 gas”, Surface and Coatings Technology, Vol. 350, pp. 863-867 which has been published in final form at https://doi.org/10.1016/j.surfcoat.2018.04.016.

This article may be used for non-commercial purposes in accordance with Elsevier for Self-Archiving

Decreased hydrogen content in diamond-like carbon grown by CH_4/Ar photoemission-assisted plasma chemical vapor deposition with CO_2 gas

Shuichi Ogawa*, Rintaro Sugimoto, Nobuhisa Kamata, and Yuji Takakuwa

Institute of Multidisciplinary Research for Advanced Materials, Tohoku University, Sendai 980-8577, Japan

* E-mail address: ogasyu@tohoku.ac.jp, Tel: +81-22-217-5367, Fax: +81-22-217-5405

Highlight

- To reduce the hydrogen concentration in DLC, CO_2 gas is added to Ar/CH_4 in photoemission-assisted plasma enhanced CVD
- Hydrogen concentration in DLC reduces with increasing CO_2 flow ratio.
- Oxygen mixing is one of the method for growth of hydrogen reduced DLC.

Abstract

In this study, we tried to decrease the hydrogen content in diamond-like carbon (DLC) grown by photoemission-assisted plasma enhanced chemical vapor deposition (PA-PECVD) using Ar/CH_4 mixed with CO_2. When the CO_2 flux was changed from 0 to 10 sccm with the Ar and CH_4 fluxes maintained at 50 and 10 sccm, respectively, the growth rate decreased from 11 to 3 μm/h. Secondary mass spectroscopy measurements confirmed that the amount of O mixed into the DLC was increased through incorporation of CO_2 into feed gas flow. The O concentration in the DLC was quantitatively evaluated by X-ray photoelectron spectroscopy (XPS) to be 0.6 atomic % at a CO_2 flow ratio of 14%. Raman spectroscopy and XPS revealed that the amount of H trapped in the DLC decreased as the CO_2 flow ratio was increased and the sp^3/sp^2 ratio remained almost unchanged. These results were interpreted by a model involving O radicals acting on the DLC surface associated with CO/CO_2 and H_2O, resulting in a decrease of the growth rate and H content. A portion of the O radicals also became incorporated into the DLC as C-O-C bonds.

1. Introduction

Diamond-like carbon (DLC) is an amorphous carbon film, featuring chemical bonds formed from a mixture of sp^3 and sp^2 carbons. This material shows hardness values ranging from 10 to 20 GPa. Amorphous carbon films containing hydrogen (a-C:H) can also become hard depending on the synthesis methods and conditions, such that a-C:H is also considered to be DLC. Physical properties such as a hardness, friction coefficient, optical band gap, and transmittance of light depend on the ratio of sp^3 and sp^2 carbons and hydrogen [1, 2]. DLC films with many sp^3 hybridized carbons are hard, and their friction coefficients become lower with increasing sp^2 bond content. The properties of DLC are controllable [3-5], such that DLC is used as a coating material for machine parts.

Methods of coating DLC can be categorized as physical vapor deposition (PVD) [6-8] or chemical vapor deposition (CVD) [9]. PVD methods involve the deposition of vaporized carbon atoms on substrates. Conversely, in CVD processes, carbon radicals, dissociated by plasma or heat are deposited on the substrates. In particular, DLC films grown by plasma enhanced CVD show good coverage of substrates with complex shapes; however, much of the soot is deposited on the process chamber wall because the plasma is usually generated in the whole chamber. Therefore, frequent maintenance and cleaning is necessary to avoid loss of quality owing to soot falling on to the substrates. In addition, DLC growth using plasma CVD cannot be performed in a clean room because the flaked soot from the chamber wall contaminates the room during exchange of substrates. Therefore, the soot prevents electronic applications of DLC films, such as in gate dielectric films for field-effect transistors (FETs) and interlayer dielectrics between the interconnects of LSI. Thus, prevention of soot deposition on the chamber wall and electrode during plasma CVD growth of DLC films is required for further applications of DLC in the electronics field.

Limiting the location of the plasma generation can reduce soot deposition because when plasma is generated on the substrate far from the chamber wall, soot is not deposited on the wall. For this purpose, we have proposed a photoemission-assisted plasma enhanced CVD (PA-PECVD) process to restrict the plasma generation to only the substrate [10-14]. PA-PECVD is a DC discharge plasma enhanced CVD process combined with UV light irradiation. Photoelectrons are emitted from the

substrate under irradiation by UV light. The photoelectrons are accelerated by the DC electric field and a plasma is generated. The photoelectrons are emitted only from the substrate such that plasma is generated only in proximity to the substrate. Soot deposition on the chamber wall is prevented because the generated photoemission-assisted (PA) plasma is generated far from the chamber wall. We expect that PA-PECVD could be used in a clean room because the soot generation of PA-PECVD is minor and we have succeeded in the fabrication of a graphene FET with a DLC gate film dielectric [14].

However, controlling the hydrogen content of DLC is also important for gate dielectric applications of DLC because the hydrogen content in gate dielectrics causes a stress-induced leakage current (SILC) [15]. To improve the SILC, the hydrogen content in a DLC should be minimized. Generally, hydrogen content in DLC grown by plasma enhanced CVD is controlled by changing the raw carbon source gases. A DLC with a high hydrogen content is grown with CH_4, which has four hydrogen atoms per carbon atom; however, C_2H_2 has only one hydrogen atom per C atom and is used for low hydrogen content DLC growth. However, only CH_4 can be used as a raw material gas for DLC growth by PA-PECVD. This restriction is attributed to the wavelength of UV light used in PA-PECVD, i.e., 172 nm (7.2 eV). These photons are absorbed by alkenes and alkynes that have low hydrogen content, resulting in their photo-dissociation [16]. The photo-dissociation of carbon hydride causes deposition of soot in the chamber. Therefore, in PA-PECVD, the feed gas composition cannot be changed to reduce the hydrogen content of the DLC films.

To address this problem, we attempted mixing oxygen into the DLC using CO_2 gas in this study. O radials were generated by mixing CO_2 gas into the PA-plasma, and the O radials abstracted hydrogen from the growing DLC surfaces. Furthermore, we expected that O atoms could passivate two C atom dangling bonds, which contribute to trapping of hydrogen, by formation of a C-O-C crosslinked structure[17]. We believe that the hydrogen content in DLC grown by PA-PECVD can be reduced with the use of CO_2 gas. CO_2 is a nontoxic and noncombustible gas, which is easier to handle than other oxide gases, such as CO and NO. To verify our hypothesis, in this study we investigated changes in the hydrogen content of DLC owing to mixing of CO_2 gas into the feed gas.

The hydrogen concentration was estimated from the photoluminescence intensity of C-H bonds in Raman spectroscopy measurements and peak fitting analysis of the C 1s peaks measured by X-ray photoelectron spectroscopy (XPS). The CO_2 flow ratio dependence of the chemical configuration was also examined by Raman spectroscopy and XPS.

2. Experimental methods

The DLC growth was performed with the use of a photoemission-assisted plasma enhanced CVD apparatus with a 3-inch sample stage. Full details of the apparatus have been described in previous works [13, 18]. A schematic illustration of the apparatus is shown in Fig. 1. The UV light was emitted from a Xe excimer lamp (UER20H-172A, USHIO: wavelength = 172 nm, power density = 50 mW/cm^2) and irradiated onto the sample through the electrode mesh. Photoelectrons were emitted not only from the sample substrate but also from the heater and holder. However, the sample was retained by a torus-shaped retainer made of quartz to allow the plasma to be generated only at the sample. The substrate was a Si wafer and the hole diameter of the quartz retainer was 16 mm.

DLC films were grown with the use of an Ar-diluted CH_4 feed gas. The fluxes of CH_4 (F_{CH4}) and Ar (F_{Ar}) were fixed at 50 sccm and 10 sccm, respectively. The flux of CO_2 (F_{CO2}) was varied from 0 to 10 sccm. Hence, the total flux ($F_{CH4} + F_{Ar} + F_{CO2}$) changed depending on F_{CO2}; however, the total pressure was maintained at 500 Pa. We define the CO_2 flow ratio R_{CO2} as $F_{CO2}/(F_{Ar} + F_{CH4} + F_{CO2})$. The Si wafer was fixed to a sample stage on a heater and the heater temperature during DLC growth was 100°C. After introducing gas into the process chamber, UV light was irradiated. Then a DC voltage of 300 V was applied between the sample and the counter electrode mesh. A uniform plasma was generated over the whole of the substrate owing to the UV irradiation, and the plasma was maintained over 10 min to grow the DLC. The discharge current was varied from 4.5 to 9.0 mA depending on the CO_2 flow ratio.

3. Results and Discussion

The CO_2 flow ratio dependence of the DLC growth rate is summarized in Fig. 2. When R_{CO2} was 0%, the growth rate was approximately 11 μm/h. This growth rate was much faster than that of PVD methods based on magnetron sputtering (2.16 μm/h)[6], laser deposition (3.6 μm/h)[7], or plasma source ion implantation (1 μm/h)[8]. However, growth rates as high as 100 μm/h have been reported for other plasma enhanced CVD methods [9], and high growth rates are a typical feature of CVD growth of DLC. Fig. 2 shows that the growth rate decreased as the CO_2 flow ratio was increased. This effect was attributed to etching of the DLC by O radicals. As the CO_2 flow ratio increased, the amount of O radials in the plasma also increased. O radials have a high chemical activity towards carbon, such that the etching rate increased as the CO_2 flow ratio was increased. However, the growth rate remained higher than 3 μm/h even at R_{CO2} = 14%. Therefore, we found that DLC films can be formed with intermixing of CO_2 gas into the feed gas.

In the next step, the oxygen concentration of the DLC films was investigated with the use of XPS and (secondary ion mass spectrometry) SIMS. In the SIMS measurements, the depth profile was measured by TOF-SIMS5-100 (Hitachi High Technology) and a Bi^+ ion beam was used as the primary ion beam. From a depth profile of the $^{16}O/^{12}C$ ratio, data from near the surface and at the interface the between DLC/Si substrate were not used to avoid the effects of adsorbent and interfacial mixing. Thus, the constant ratio in the central region of DLC films was adopted. The DLC surface was sputtered by Ar^+ ions before XPS measurements to remove surface adsorbed H_2O and other contamination. The XPS measurements were performed with the use of a PHI5000 VersaProbe II (Ulvac-phi), and the X-ray energy was 1486.6 eV. In the XPS measurements, the O 1s and C 1s photoelectron intensities were interpreted with the following equations:

$$I_C = I_0 n_C \sigma_C \int_0^{\infty} exp\left(-\frac{x}{\lambda_C}\right) dx \ , \qquad (1)$$

$$I_O = I_0 n_O \sigma_O \int_0^{\infty} exp\left(-\frac{x}{\lambda_O}\right) dx \ , \qquad (2)$$

where, I_0, n_C, n_O, σ_{C1s}, σ_{O1s}, λ_{C1s}, and λ_{O1s} are the intensity of X-rays, atomic density of carbon and oxygen in the DLC, the ionization cross-section of the C 1s and O 1s orbitals, and the inelastic mean

free path of C 1s and O 1s photoelectrons in the DLC films, respectively. Using these equations, we calculated the oxygen concentration in the DLC films as follows:

$$\frac{n_O}{n_C} = \frac{I_O \sigma_C \lambda_C}{I_C \sigma_O \lambda_O} \ . \qquad (3)$$

The values of photoionization were $\sigma_{C1s} = 1.3\times10^{-2}$ Mb, $\sigma_{O1s} = 4.0\times10^{-2}$ Mb, respectively [19]. The inelastic mean free path in DLC has not yet been reported, hence, we adopted values from diamond [20]. The X-ray energy was 1486.6 eV; thus, the kinetic energies of the C 1s and O 1s photoelectrons were approximately 1202 and 956 eV, respectively. The actual values were obtained by linear approximation from the database [20], and we used the values of $\lambda_{O1s} = 15.8$ nm and $\lambda_{C1s} = 18.8$ nm.

The results of the CO_2 flow ratio dependence of the oxygen content in the DLC films, measured by SIMS and XPS, are summarized in Fig. 3. The measurement depths of SIMS and XPS are different; however, both results showed a linear increase of the oxygen concentration as the CO_2 flow ratio was increased. This result indicates that O atoms do not agglomerate but are uniformly distributed in the DLC. The XPS measurements provide a quantitative estimate of the oxygen concentration. The oxygen concentration increased up to 0.6 atomic% at $R_{CO2} = 14\%$. Thus, we were able to grow oxygen-containing DLC using CO_2 gas.

Evaluation of the hydrogen content in the DLC and its chemical configuration was performed by Raman spectroscopy with a Nano finder TERS (Tokyo Instruments) and an excitation laser wavelength of 532 nm. When the DLC contained hydrogen, a broad peak from photoluminescence (PL) owing to C-H bonds appeared under laser irradiation. The width of the PL peak was broader than the wavelength region measured in Raman spectroscopy, such that the PL peak was observed as a background in the Raman spectra. Therefore, the background slope could be used for the qualitative estimation of the hydrogen content in DLC[21]. The Raman spectra of the oxygen-containing DLC samples grown by changing the CO_2 flow ratio are shown in Fig. 4. Generally, DLC features two peaks in its Raman spectra, namely a G peak derived from stretching vibration of C-C sp^2 bonds and a D peak derived from radial breathing vibrations of six-membered rings. Additionally, it has recently been reported that the D band of DLC, including nanocrystalline graphite, has two components [22,

23]. We also used the two components D_A and D_S of the D peak of DLC to obtain the most suitable fitting results. The background level was assumed to be the base of the PL peak derived from the C-H bonds, such that a linear approximation was used as the background. Hence, we assumed that the intensity of the PL peak was proportional to background slope. The CO_2 flow ratio dependence of the background slope is shown in Fig. 4(b). The CO_2 flow ratio dependence of the D = (D_S + D_A)/G intensity ratio is also shown in Fig. 4(c). The D/G intensity ratio was constant or slightly decreased depending on the CO_2 flow ratio.

To confirm the hydrogen concentration in the DLC, XPS peak fitting analysis performed. The C 1s photoelectron spectra at R_{CO2} = 0% and 14% are shown in Fig. 5(a). The C 1s photoelectron spectra could be divided into two components attributed to sp^2 and sp^3 bonds. The peak intensity ratios between the sp^2 and sp^3 components are shown in Fig. 5(b). The sp^3/sp^2 ratio decreased as the CO_2 flow rate was increased. As shown in Fig. 4(c), the D/G ratio was constant or decreased slightly. The decrease of the D/G ratio indicated a decrease of sp^3 bonding in the DLC. Therefore, the XPS results showed good agreement with those from Raman spectroscopy. The sp^3 component in the XPS included not only C-C but also C-H bonds, which were indistinct [24, 25]. The sp^3/sp^2 C-C bond ratio was almost constant or slightly decreased, as shown in Fig. 4(c); however, the sp^3/sp^2 components decreased considerably as shown in Fig. 5(b). This result indicates that the number of C-H bonds decreased as the CO_2 flow rate was decreased.

Finally, we discuss the changes to the electrical properties of the DLC induced by the oxygen content. As shown in Fig 3, the oxygen content of the DLC increased linearly with the CO_2 flow ratio. However, it has been reported that both the dielectric constant and dielectric breakdown strength remain constant regardless of the amount of oxygen in the DLC[17]. However, the background slope and sp^3/sp^2 bonding ratio decreased when R_{CO2} > 4%. This result indicates that the number of C-H bonds in the DLC, i.e., the hydrogen concentration in the DLC, decreased under a greater CO_2 flow. We found that the hydrogen content could be reduced by adding CO_2 gas into PA-PECVD.

On the basis of the above results, we propose a hydrogen reduction model for DLC synthesized with $Ar/CH_4/CO_2$ gases in PA-PECVD. When CO_2 is not mixed with the raw gas or the CO_2 flow

ratio is small, sputtering by Ar^+ ions is the main process leading to removal of H atoms terminating the DLC surfaces. When there are H atoms terminating the DLC surface, Ar^+ ions in the plasma collide with the DLC surface and enhance desorption of the H atoms. However, the desorbed H atoms remain chemically active, such that H atoms adsorb again onto the DLC surface or dangling bonds in the DLC. Therefore, the removal efficiency is not high. As a result, many H atoms remain in the DLC under a low CO_2 flow ratio. However, O radicals are generated in the plasma when CO_2 is mixed with the raw gas. The O radials abstract terminated H atoms, which then desorb from the DLC surfaces as OH or H_2O molecules. Furthermore, O atoms can bond with two atoms unlike H atoms. Therefore, O radials can form C-O-C bridge structures [16] and passivate dangling bonds. The oxygen concentration in the DLC increases together with the CO_2 flow ratio, as shown in Fig. 3. The O atoms prevent re-adsorption of hydrogen by passivating dangling bonds. As the result, the H concentration in the DLC is decreased.

4. Conclusion

In DLC synthesis using photoemission-assisted plasma enhanced CVD, the hydrogen concentration of DLC films can be reduced by mixing of CO_2 into the CH_4/Ar feed gases. This mixing is thought to result in O radicals generated from CO_2 that enhance the desorption of surface-terminated hydrogen by forming OH or H_2O molecules. Furthermore, re-adsorption of desorbed hydrogen at dangling bonds of carbon atoms is also suppressed because O atoms in the DLC form C-O-C bridge structures. In this structure, one O atom can passivate the dangling bonds of two carbon atoms. As described above, the hydrogen concentration in the DLC can be reduced with the use of CO_2. Therefore, we conclude that DLC with a low hydrogen content can be synthesized by photoemission-assisted plasma enhanced CVD, for which only CH_4 can be used as a raw feed gas for the DLC growth.

Acknowledgement

This work was supported by the Japan Society for the Promotion of Science (JSPS) KAKENHI Grant Number JP16K14124. This work was supported in part by “Dynamic Alliance for Open Innovation

Bridging Human, Environment and Materials" from the Ministry of Education, Culture, Sports, Science and Technology of Japan (MEXT).

References

[1] W. Jacob and W. Mller, J. Appl. Phys. **63** (1993) 1771-1773.

[2] A. C. Ferrari and J. Robertson, Phys. Rev. B **61** (2000) 14095-14107.

[3] J. Robertson, Mater. Sci. Eng. R **37** (2002) 129-281.

[4] K. A. H. Mahmud, M. A. Kalam, H. H. Masjuki, H. M. Mobarak and N. W. M. Zulkifli, Crit. Rev. Sol. State Mater. Sci, **40** (2015) 90-118.

[5] Y.Liu, A. Erdermir, and E.I. Meletis, Surf. Coat. Tech. **82** (1996) 48-56.

[6] F. Garrelie, A. S. Loir, C. Donnet, F. Rogemond, R. Le Harzic, M. Belin, E. Audouard, and P. Laporte, Surf. Coat. Tech. **163–164** (2003) 306–312.

[7] R. D. Mansano, M. Massi, L. S. Zambom, P. Verdonck, P. M. Nogueira, H. S. Maciel, and C. Otani, Thin Solid Films, **373** (2000) 243–246.

[8] S. M. Malik, R. P. Fetherston, and J. R. Conrad, J. Vac. Sci. Technol. A, **15** (1997) 2875–2879.

[9] H. Kousaka, T. Okamoto, and N. Umehara, IEEE Trans. Plasma Sci. **41** (2013) 1830-1836.

[10] T. Takami, S. Ogawa, H. Sumi, T. Kaga, A. Saikubo, E. Ikenaga, M. Sato, M. Nihei, and Y. Takakuwa, e-J. Surf. Sci. Nanotechnol. **7** (2009) 882-890.

[11] H. Sumi, S. Ogawa, M. Sato, A. Saikubo, E. Ikenaga, M. Nihei, and Y. Takakuwa, Jpn. J. Appl. Phys. **49** (2010) 076201.

[12] M. Yang, S. Ogawa, S. Takabayashi, T. Otsuji, and Y. Takakuwa, Thin Solid Films **523** (2012) 25-28.

[13] M. Kawata, Y. Ojiro, S. Ogawa, T. Masuzawa, K. Okano, and Y. Takakuwa, J. Vac. Sci. Technol. A **32** (2014) 02B110.

[14] S. Takabayashi, S. Ogawa, Y. Takakuwa, H.C. Kang, R. Takahashi, H. Fukidome, M. Suemitsu, and T. Otsuji, Diamond Relat. Mater. **22** (2012) 118-123.

[15] Y. Mitani, H. Satake and A. Toriumi, IEEE Int. Electron Devices Meet., Tech. Dig., (2001) 129–132.

[16] K. Watanabe, J. Chem. Phys. **40** (1964) 558.

[17] S. Takabayashi, M. Yang, T. Eto, H. Hayashi, S. Ogawa, and Y. Takakuwa, Diamond Relat. Mater. **53** (2015) 11-17.

[18] M. Yang, S. Takabayashi, S. Ogawa, H. Hayashi, R.Ješko, T. Otsuji, and Y. Takakuwa, Jpn. J. Appl. Phys. **52** (2013) 110123.

[19] J. J. Yeh and I. Lindau, At. Data Nucl. Data Tables **32** (1985) 1-155.

[20] S. Tanuma, C. J. Powell, and D. R. Penn, Surf. Interface Anal. **43** (2011) 689-713.

[21] C. Casiraghi, A. C. Ferrari, and J. Robertson, Phys. Rev. B **72** (2005) 085401.

[22] J. Ribeiro-Soares, M.E. Oliveros, C. Garin, M.V. David, L.G.P. Martins, C.A. Almeida, E.H. Martins-Ferreira, K. Takai, T. Enoki, R. Magalhaes-Paniago, A. Malachias, A. Jorio, B.S. Archanjo, C.A. Achete, L.G. Cançado, Carbon **95** (2015) 646-652.

[23] S. Takabayashi, R.Ješko, M. Shinohara, H. Hayashi, R. Sugimoto, S. Ogawa, and Y. Takakuwa, Surf. Sci. **668** (2018) 36–41.

[24] J.C. Lascovich and S Scaglione, Appl. Surf. Sci. **78** (1994) 17-24.

[25] S. Ogawa, T. Yamada, S. Ishizduka, A. Yoshigoe, M. Hasegawa, Y. Teraoka, Y. Takakuwa, Jpn. J. Appl. Phys. **51** (2012) 11PF02.

Figure captions

Fig. 1. Schematic illustration of photoemission-assisted plasma enhanced CVD apparatus and photograph of DLC grown on a Si substrate.

Fig. 2. CO_2-flow ratio dependence of the DLC growth rate.

Fig. 3. CO_2-flow ratio dependence of (a) $^{16}O/^{12}C$ intensity ratio measured by SIMS and (b) oxygen concentration measured by XPS.

Fig. 4. (a) Raman spectra of DLC. The spectra can be fitted by three peaks and a linear background. CO_2-flow ratio dependence of (b) background slope of the Raman spectra and (c) D/G peak intensity ratio.

Fig. 5. (a) C 1s photoelectron spectra of DLC grown with CO_2 flow rates of 0% and 14.3%. (b) CO_2-flow rate dependence of sp^3/sp^2 ratio obtained from XPS.

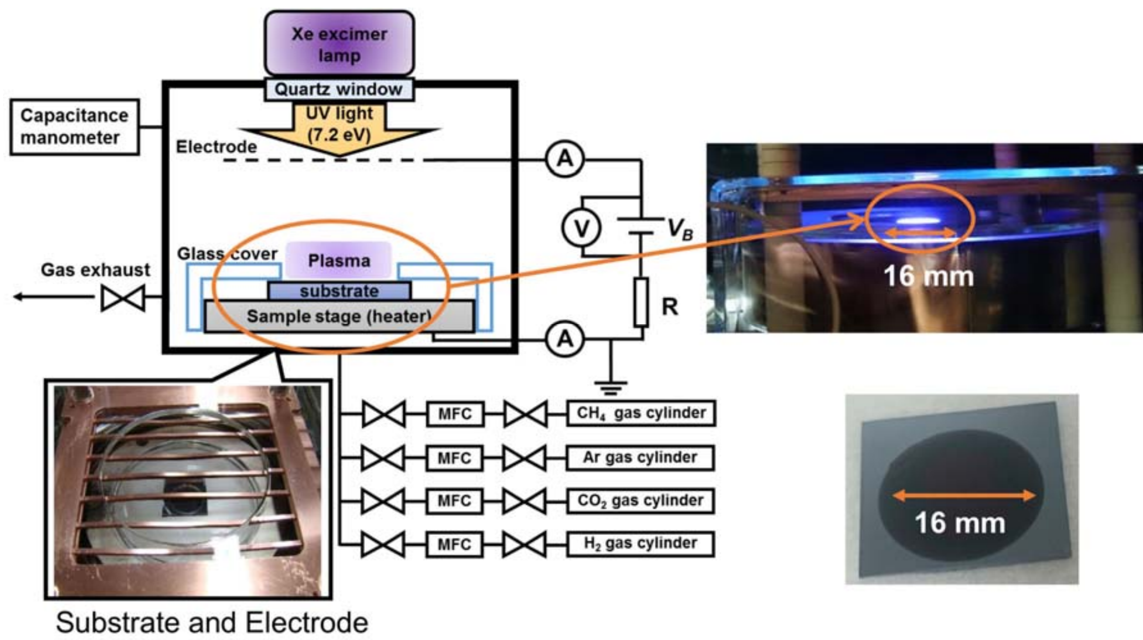

Fig. 1

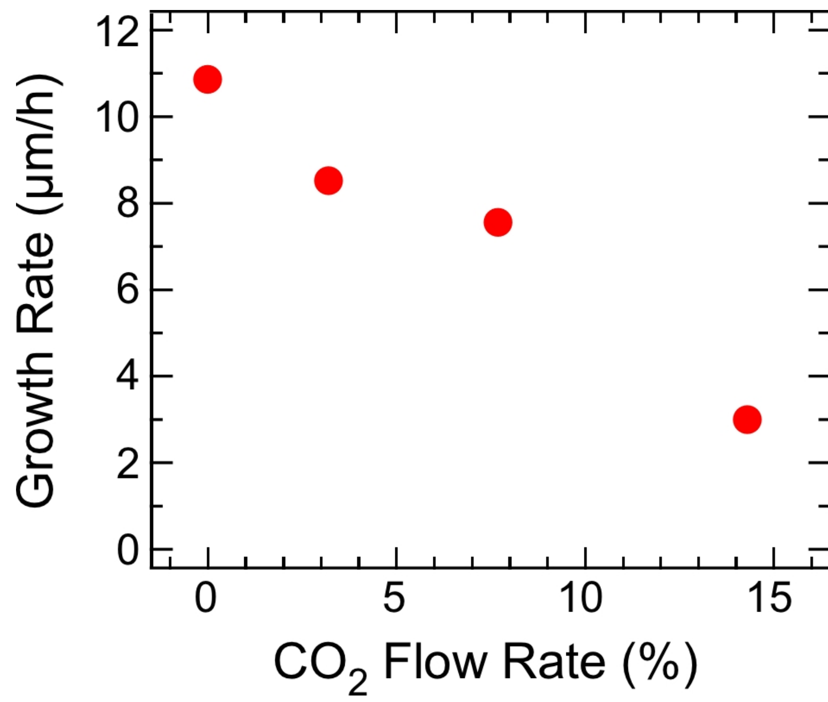

Fig. 2

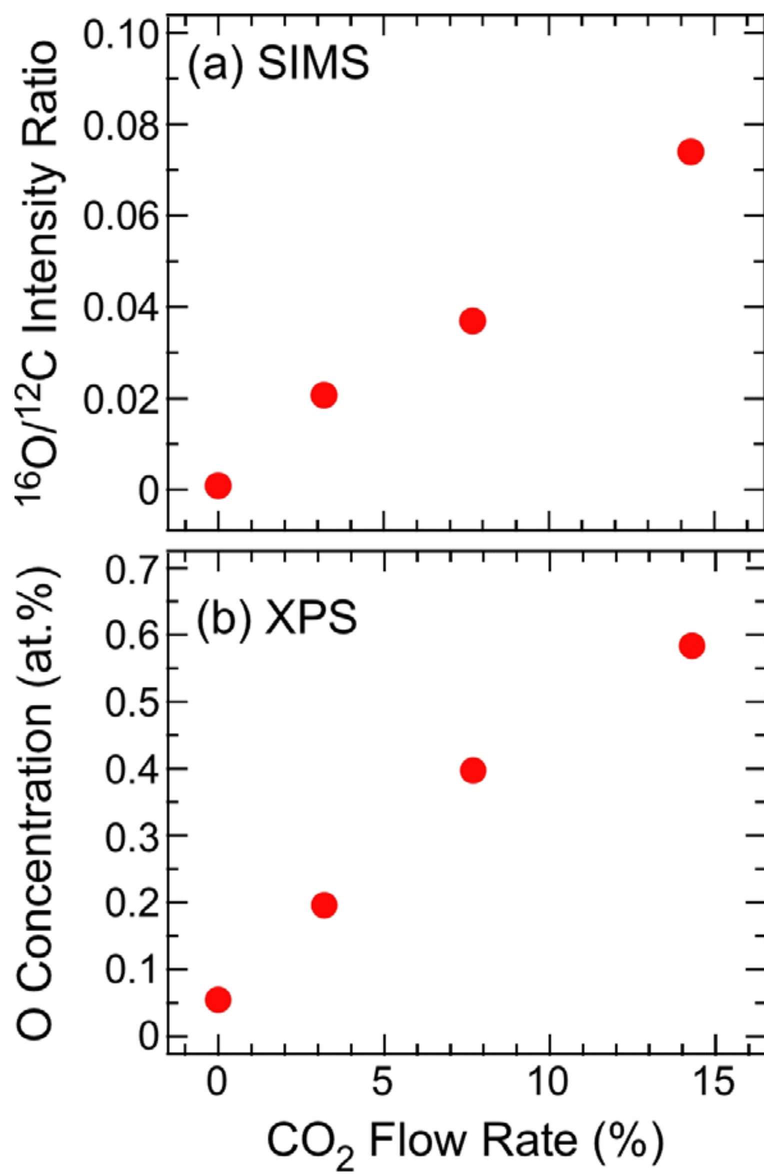

Fig. 3

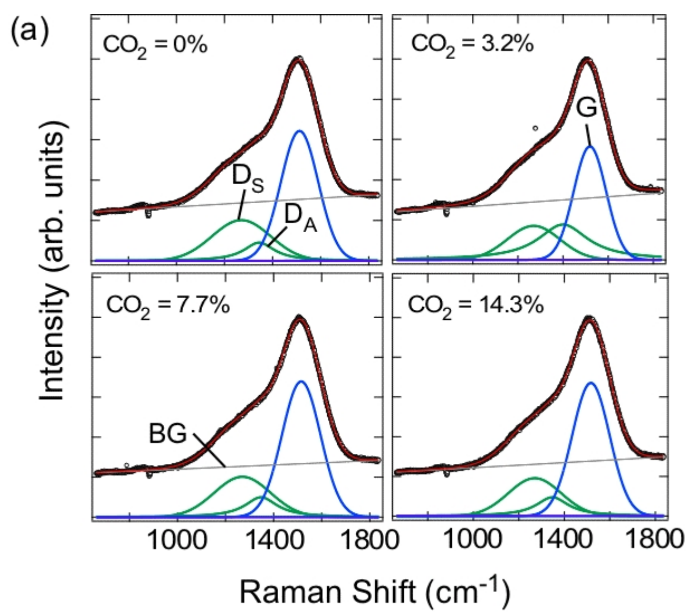

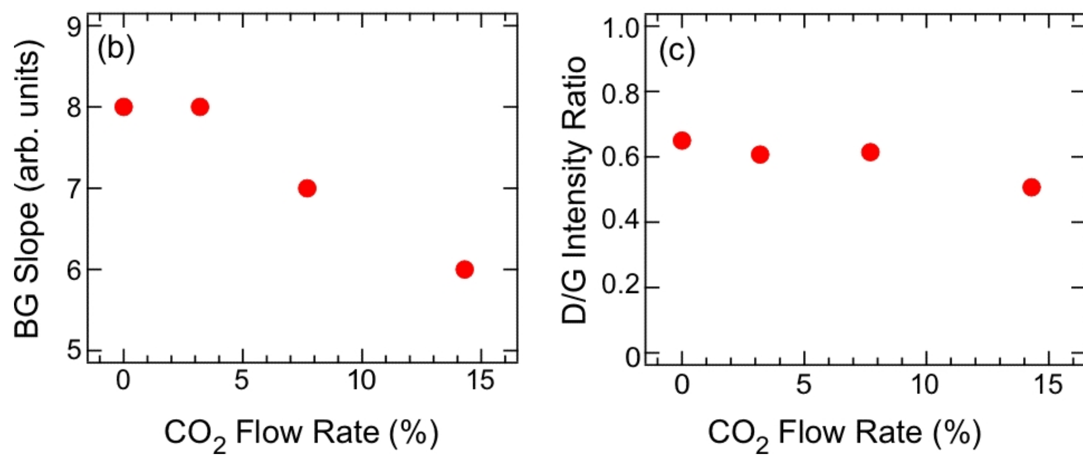

Fig. 4

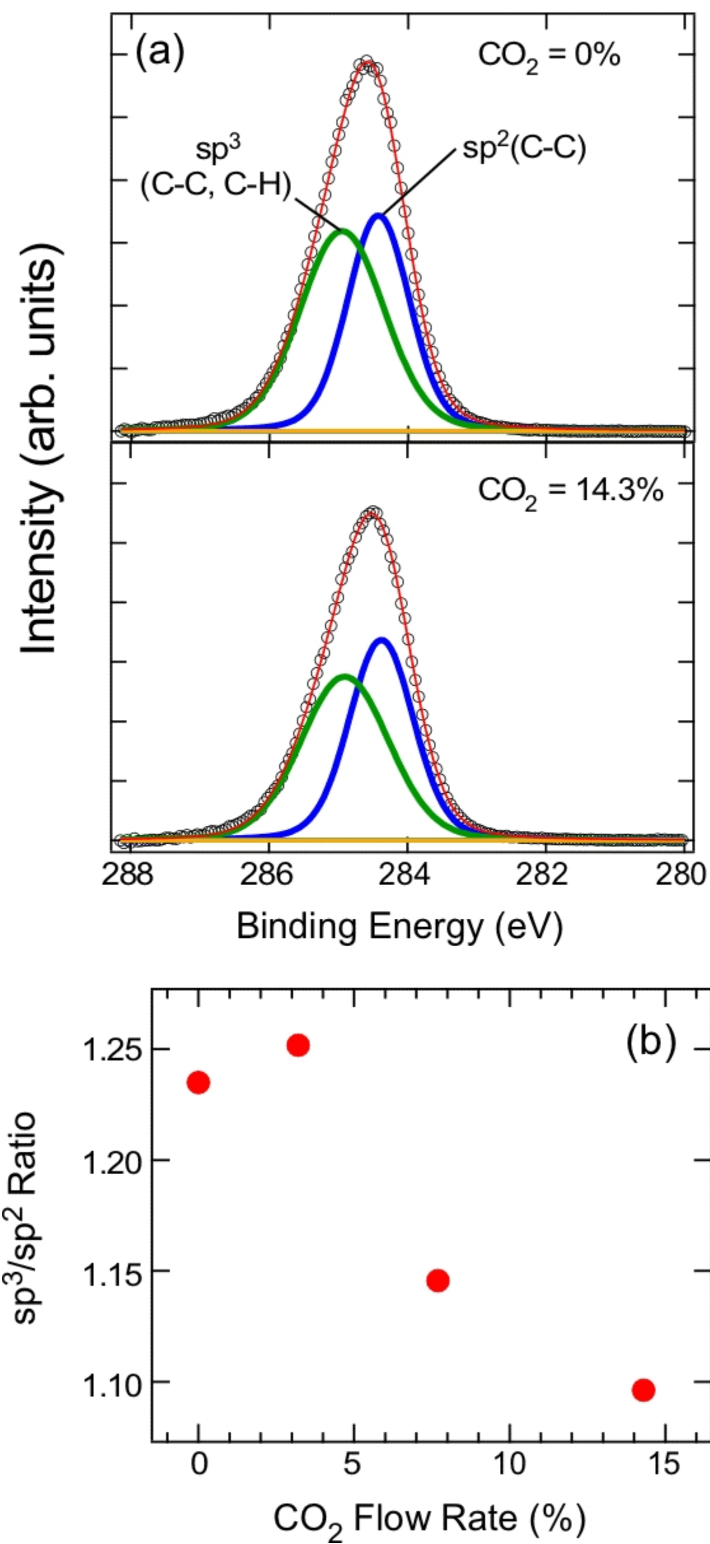

Fig. 5